JMEPEG (2024) 33:6380–6386
https://doi.org/10.1007/s11665-024-09334-5

1059-9495/$19.00

ORIGINAL RESEARCH ARTICLE

Metallurgical and Mechanical Properties of Friction Stir-Welded Pure Titanium

Michael Regev and Stefano Spigarelli

Submitted: 12 September 2023 / Revised: 21 December 2023 / Accepted: 14 February 2024 / Published online: 14 March 2024

Commercially pure titanium (CP-Ti) plates were friction stir welded (FSWed) using a welding tool with a tungsten carbide (WC) pin. The bead-on-plate technique was applied to reduce the effects of welding defects, such as incomplete penetration. Whereas many papers have reported on creep studies of CP-Ti as well as on FSW of CP-Ti, no paper has investigated the creep behavior of a CP-Ti FSW'ed joint. Consequently, the current study focuses on this topic. The current paper, which is part of a broader research project, focuses on the metallurgical processes occurring during the creep of a FSW'ed CP-Ti joint at the temperature range of 550-650 °C. Based on the current study and previous results obtained by the authors, it can be concluded that the weld is not the weakest link. In every case, necking and creep fracture occurred in the parent material (PM), rather than either the thermomechanically affected zone (TMAZ) or the stir zone (SZ), indicating that both zones are more creep-resistant than the parent material. Fractography showed that the fracture surface was typical of creep fracture and that the fracture mechanism was microvoid coalescence and also ruled out any preexisting defect. TEM study of broken crept specimens revealed randomly distributed dislocations but no evidence of grain refinement, hence leading to the conclusion that dislocation glide was the dominant creep mechanism. The technological implication of the current study is that the welding process is safe for use as far as its creep properties are concerned.

Keywords CP-Ti, dislocations, friction stir welding, mechanical properties, microstructure

1. Introduction

Titanium and its alloys are known for their high specific strength, high heat resistance, high erosion and corrosion resistance (Ref 1-11). Because friction stir welding (FSW) is a non-fusion joining process, it avoids the metallurgical problems associated with fusion and re-solidification. Among these, problems are grain coarsening, porosity and formation of brittle coarse cast structure and Ti oxide, in addition to residual stresses and distortion (Ref 1-7). Nevertheless, applying FSW to Ti and its alloys is somewhat challenging due to its high melting temperature (1668 °C), thus requiring more temperature wear-resistant welding tool materials (Ref 3, 7-9, 12-17).

Several studies have examined the microstructure obtained during the FSW of Ti (Ref 1-9, 12-19). Yet these studies are marked by many discrepancies, including the sizes and shapes of the grains in the different zones and the presence of various zones in the vicinity of the weld. However, the researchers seem to agree that the development of the microstructure during FSW is a multistage complicated process as stated by Sajid et al. in their review (Ref 19). In light of the discrepancies mentioned, the authors carried out an independent comprehensive microstructure study as a preliminary step (Ref 20). That preliminary study focused on the mechanical properties, namely tension and hardness, as well as on fractography. It also included a quantitative transmission electron microscopy (TEM) study that compared the parent material and the stir zone of FSW'ed commercially pure (CP) Ti. One of the results reported in that paper was that the mechanical properties of the FSW'ed material at room temperature were not inferior to those of the parent material. Another finding was the detection of grain refinement and mechanical twinning inside the TMAZ and the stir zone. This grain refinement was related to dynamic recrystallization (DRX) occurring during FSW. The results of the fractography study showed that in both cases—namely, the parent and the FSW'ed material—the fracture had the same ductile character.

Many creep studies of CP-Ti have been conducted at ambient temperatures as well as at high temperatures. Several of these studies (Ref 21-26) refer to metallurgical processes occurring during creep of CP-Ti at high temperatures. For example, Pushp et al. (Ref 21) mentioned the high creep resistance of Ti and its alloys, and Gangwar and Ramulu (Ref 22) pointed to 550 °C as the upper limit for high temperature applications. Dvorak et al. (Ref 23, 24) studied creep resistance of CP-Ti with different grain sizes, starting from 0.2-0.25 μm up to 1.75 μm, at temperatures of up to 450 °C. They reported additional grain coarsening up to about 2 μm and dislocation recovery occurring during creep. Dvorak et al. (Ref 23, 24)

This article is an invited submission to the *Journal of Materials Engineering and Performance* selected from presentations at the symposium "Joining," belonging to the area "Processing" at the 17th European Congress and Exhibition on Advanced Materials and Processes (EUROMAT 2023), held in Frankfurt am Main, Germany, from September 3 to September 7, 2023.

Michael Regev, Department of Mechanical Engineering, Braude College, P.O. Box 78, 21982 Karmiel, Israel; and **Stefano Spigarelli**, DIISM, Università Politecnica delle Marche, 60131 Ancona, Italy. Contact e-mail: michaelr@braude.ac.il.

reported improved creep resistance of the submicron grain size material compared to materials with coarser grain size. Based on stress exponent and activation energy calculations, Dvorak et al. (Ref 23, 24) claimed that dislocation creep can be regarded as the dominant creep mechanism. Long et al. (Ref 25) examined the compressive deformation behavior of CP-Ti with ~ 35 μm average grain size versus the same material with ~ 250 nm average grain size at temperatures of up to 600 °C. They pointed out the contribution of grain boundary sliding and Coble-type creep in the case of the ~ 250 nm grained material at 600 °C. Matsunaga et al. (Ref 26) studied the creep behavior of CP-Ti with an average grain size of 75 μm at temperatures of up to 600 °C. Their TEM yielded planar dislocation arrays due to planar glide without tangling.

Although, as stated earlier, both creep and FSW studies of CP-Ti have been conducted and published, to the best of the authors' knowledge, no study to date has examined the creep behavior of a FSW'ed joint. Ganesan and Pothur (Ref 17) also mentioned the lack of creep studies of friction stir-welded Ti and Ti alloys. In order to fill this gap in the literature, the authors focused on this topic in their current study. They chose to use bead-on-plate specimens rather than "real" butt-welded specimens in order to rule out the influence of certain FSW defects, such as incomplete penetration, on the mechanical properties, thereby ensuring that the mechanical properties would be dictated solely by the microstructural changes.

The current paper, which is a part of a broader research project, focuses on the metallurgical processes occurring during the creep of a FSW'ed CP-Ti joint. As stated earlier, the microstructure and mechanical properties of the FSW'ed joint were the subject of a previous publication by the authors (Ref 20), while an analytical study of the creep process was published elsewhere (Ref 27). The current paper describes and discusses a TEM study of crept specimens together with fractography and metallurgical studies of FSW'ed CP-Ti. The practical conclusion of the current study is that similar to the room temperature (RT) mechanical properties of the welded joint, the creep resistance of the welded joint is not inferior to that of the parent material. This means, in turn, that the FSW of CP-Ti has the potential to be safe for use at both RT and high temperatures.

2. Experimental Procedure

The material used for this study was grade 2 CP-Ti in the form of plates measuring 200 mm × 200 mm plates, 3 mm thick. These plates were subjected to bead-on-plate FSW using a M32 CNC milling machine (Sharnoa Computerized Machines Ltd., Petah Tikva, Israel). Bead-on-plate was applied instead of real weld to ensure that the mechanical behavior was solely related to metallurgical processes rather than to defects in welding. The welding tool was made of H-13 tool steel with a 20-millimeter-diameter shoulder and a 2-millimeter-long WC pin. The FSW process optimization, which was reported elsewhere (Ref 20), was relatively complicated due to the high temperatures developing during welding. These high temperatures, in turn, accelerate the wear process of the welding tool. After approximately 160 mm of welding, the shoulder of the welding tool developed a mushroom shape, as shown in Fig. 1. Therefore, each welding tool was replaced after 80 mm of welding to avoid the influence of shoulder deformation.

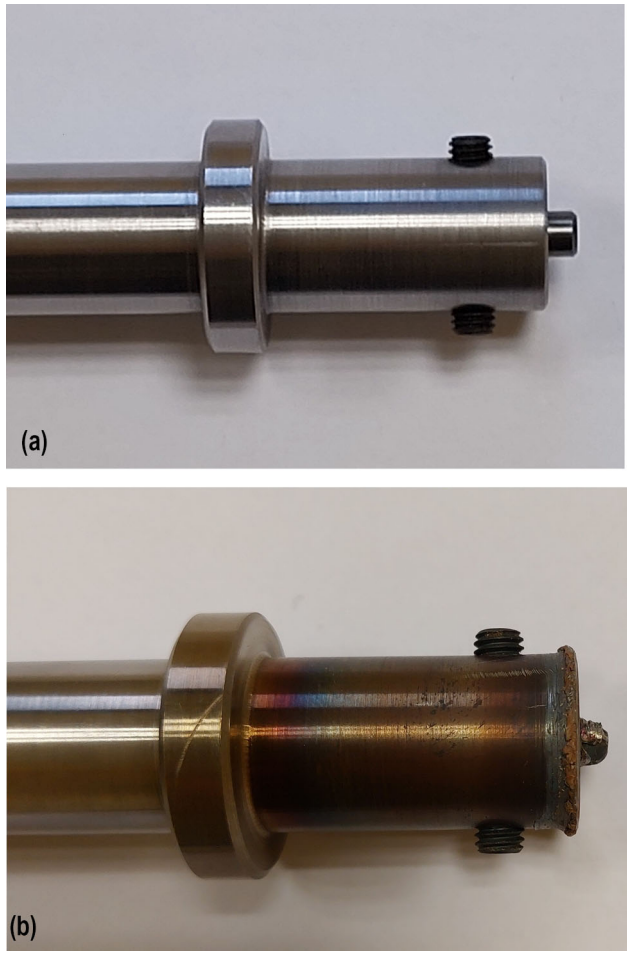

Fig. 1 The welding tool: (a) new (b) worn out

Rotational speed of $\omega = 700$ rpm and a transverse speed of $v = 50$ mm/min were chosen as the welding parameters. The welding was carried out under an Ar protective atmosphere.

Creep specimens with a square cross section measuring 3 mm × 3 mm and a gauge length of 25 mm were machined from the FSW region of the plates. The longitudinal axis of the samples was perpendicular to the FSW direction, as shown in Fig. 2. Creep tests were conducted on these specimens at 550, 600 and 650 °C.

The TEM investigation was conducted using an FEI Tecnai G2 T20 TEM. TEM specimens were prepared using a Thermo Fisher Helios 5 CX PFIB (plasma focused ion beam). The fractography study was conducted on broken friction stir-welded creep specimens with the aid of an FEI Inspect SEM.

3. Results and Discussion

Figure 3 depicts two typical creep curves. Figure 3(a) shows parent material crept under 40 MPa at 550 °C, and Fig. 3(b) shows FSW'ed material crept under 90 MPa at 550 °C. These curves are presented here to give an overview of the different creep resistances and times to fracture of the parent material and the FSW'ed material at a given temperature. It should be noted that the current paper does not focus on the creep behavior. For a comprehensive study of the creep response of

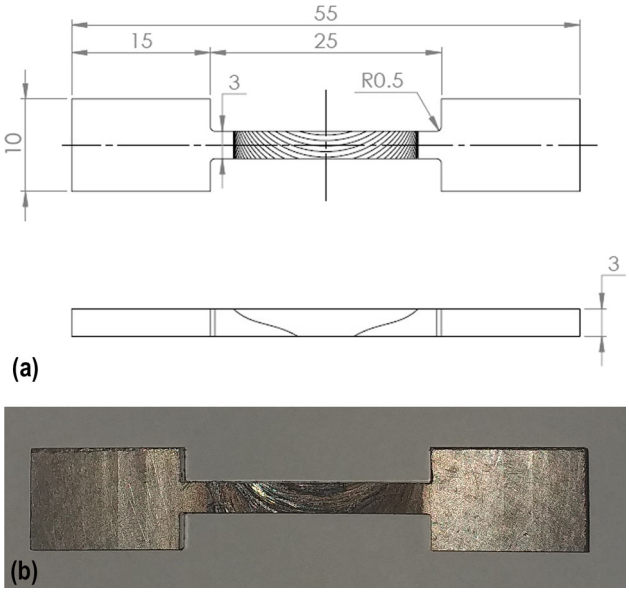

Fig. 2 Creep specimen: (a) drawing; (b) image

FSW'ed material, see a recent publication by the authors (Ref 27).

According to Mishra and Mahoney (Ref 28), when the research in the field of FSW was extended to alloys other than Al ones (unlike A1 alloys, in these other alloys three distinct zones—SZ, HAZ and TMAZ—are not clearly observable), the FSW licensees group recommended to redefine the TMAZ. According to this new definition, the TMAZ includes all regions affected by both heat and deformation with the SZ subset within the TMAZ. The authors of this paper found the new definition more appropriate for the current case and therefore use it in this discussion. However, it should be noted that some researchers, like Singh et al. (Ref 16), continue to distinguish between the SZ and the TMAZ of Ti to this day.

In all cases, creep fracture occurred at the parent material and not at the TMAZ. Figure 4(a) shows a front view of a broken FSW'ed specimen that underwent creep under 112 MPa at 550 °C, and Fig. 4(b) shows its side view. The TMAZ is clearly indicated in Fig. 4(b) while all the rest of the specimen is the BM. These figures show that both necking and fracturing occurred outside the TMAZ, while a second neck can be seen on the opposite side of the TMAZ. This "double necking" at

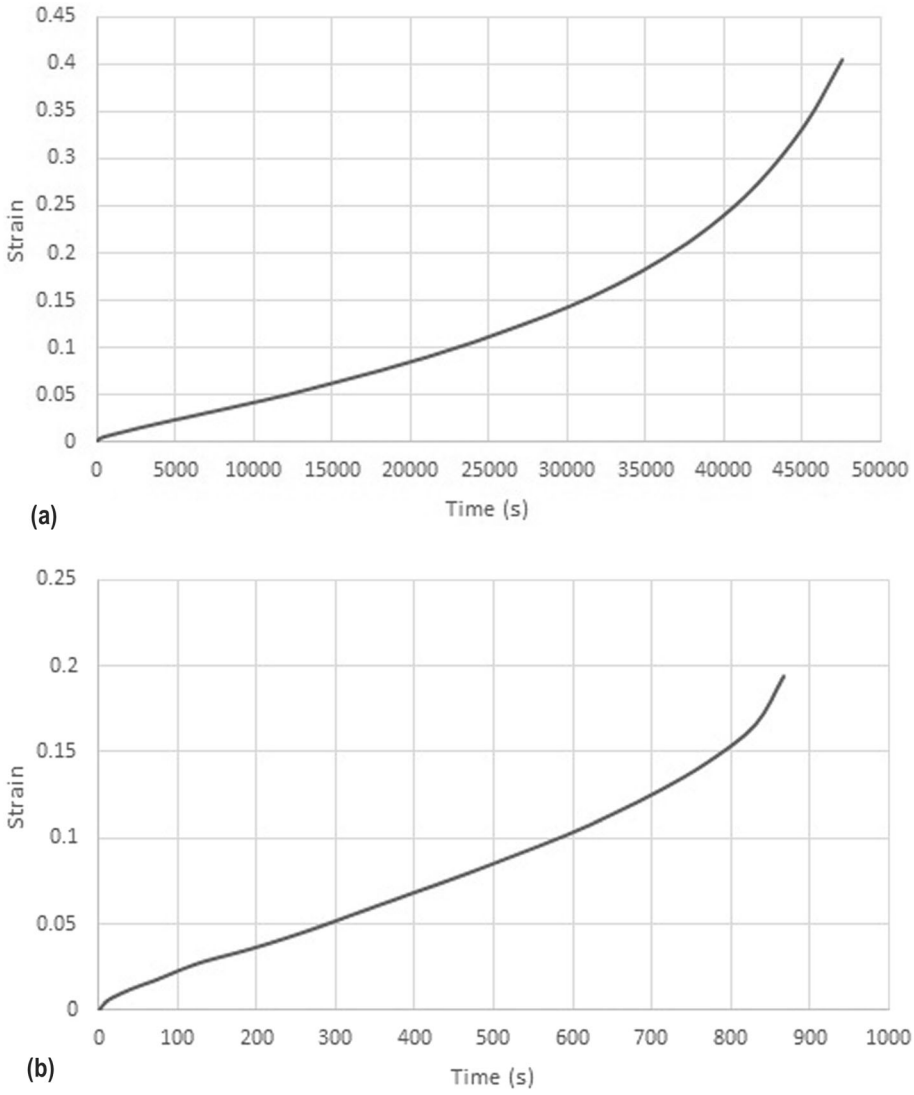

Fig. 3 Creep curves at 550 °C: (a) Parent material under 40 MPa; (b) FSW'ed material under 90 MPa

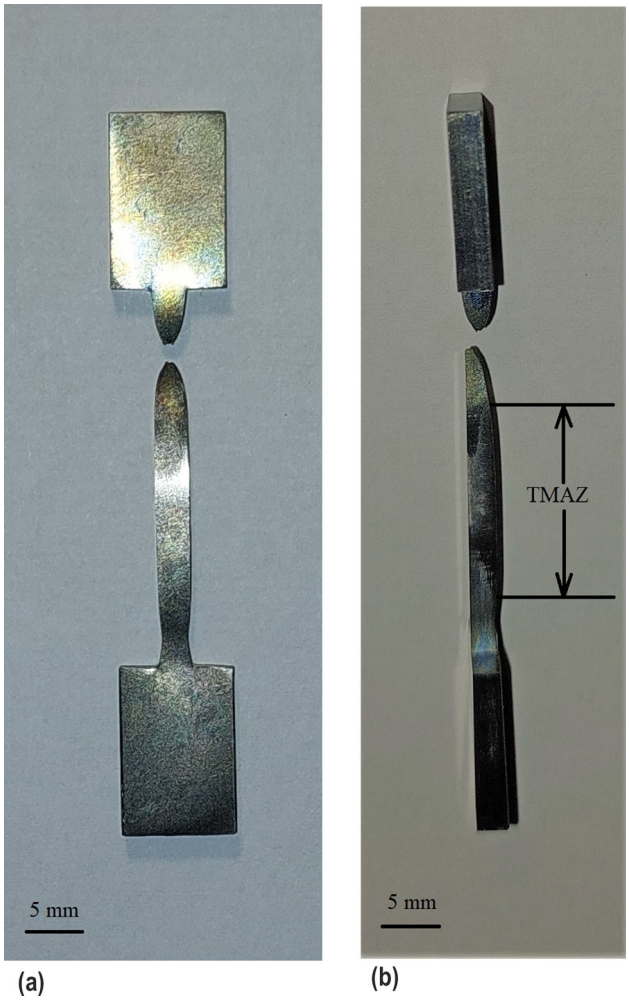

Fig. 4 A broken specimen that underwent creep under 112 MPa at 550 °C: (a) front view; (b) side view

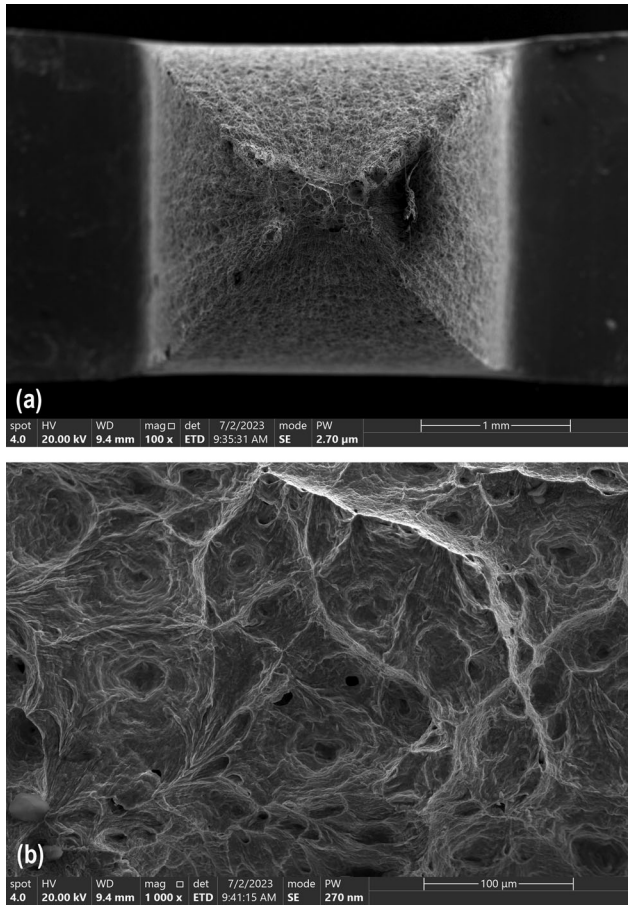

Fig. 5 An SEM micrograph of a specimen that underwent creep under 112 MPa at 550 °C: (a) general view; (b) fracture surface

the parent material—in addition to fracture—shows that at the temperature range studied, the TMAZ is more creep resistant than the parent material. Furthermore, since TMAZ is more creep resistant, it should not be regarded as the weak link, and creep properties are determined by the parent material. Therefore, the TEM study was carried out on the parent material, in which creep deformation is primarily localized.

Figure 5(a) is an SEM micrograph providing a general view of the fracture surface of the broken creep specimen shown in Fig. 4, whereas the SEM micrograph shown in Fig. 5(b) was taken under higher magnification. The fracture surface of the creep specimen is homogeneous and fully dimpled, as can be seen in Fig. 5(b). Moreover, Fig. 5(b) shows that the fracture occurred by microvoid coalescence, which, in turn, is typical of creep fracture. The surfaces of all the fracture specimens observed, showed no evidence of preexisting cracks or other defects.

Figure 6(a) depicts a BF image of the TMAZ of a FSW'ed specimen prior to creep, for a detailed TEM study of the FSW'ed material versus the raw material the reader is referred to (Ref 20). However, Fig. 6(a) is provided here for the sake of comparison with Fig. 7(a), while the selected area diffraction pattern (SADP) taken from the region of interest (ROI) depicted in Fig. 6(a) is shown in Fig. 6(b). Figure 7(a) and (b) shows bright field (BF) TEM micrographs of the parent material of a specimen that underwent creep under 12 MPa at 650 °C taken near $< 5\bar{1}43 >$ z.a., while Fig. 7(c) shows the indexed SADP of $< 5\bar{1}43 >$ z.a.

As reported by the authors (Ref 20), the grains of the parent metal were equiaxed, with an average size of about 20-30 μm, while the TMAZ was found to be made of fine equiaxed dislocation free grains having an average size of less than 100 nm, as can be seen in Fig. 6a. The electron SADP of the shown in Fig. 6b, with its rings composed of many sharp spots shows evidence of the material being nano-crystalline. This grain size measure is also in good agreement with Liu et al. (Ref 19). The existence of such ultrafine grains was attributed to dynamic recrystallization (DRX). Contrary to Fig. 6a, the entire regions of interest (ROI) depicted in Fig. 7(a) and (b) belong to one single grain as can be seen from their SADP shown in Fig. 7(c). Figure 7(a) also shows randomly distributed dislocations as indicated by arrows, while Fig. 7(b) depicts a dislocation structure as indicated by arrow 1 together with scattered dislocations as indicated by arrows 2, but no evidence of grain refinement is apparent. The dislocation structures, like the one shown in Fig. 7(b) are likely sub-grain walls in their formation stage. It should be noted that the specimen from which Fig. 7 were taken had been strained by about 18%, thus, plastic deformation and temperature exposure during creep were not sufficient to induce DRX. The absence of sub-grain structures in crept specimens is consistent with the finding of Matsunaga

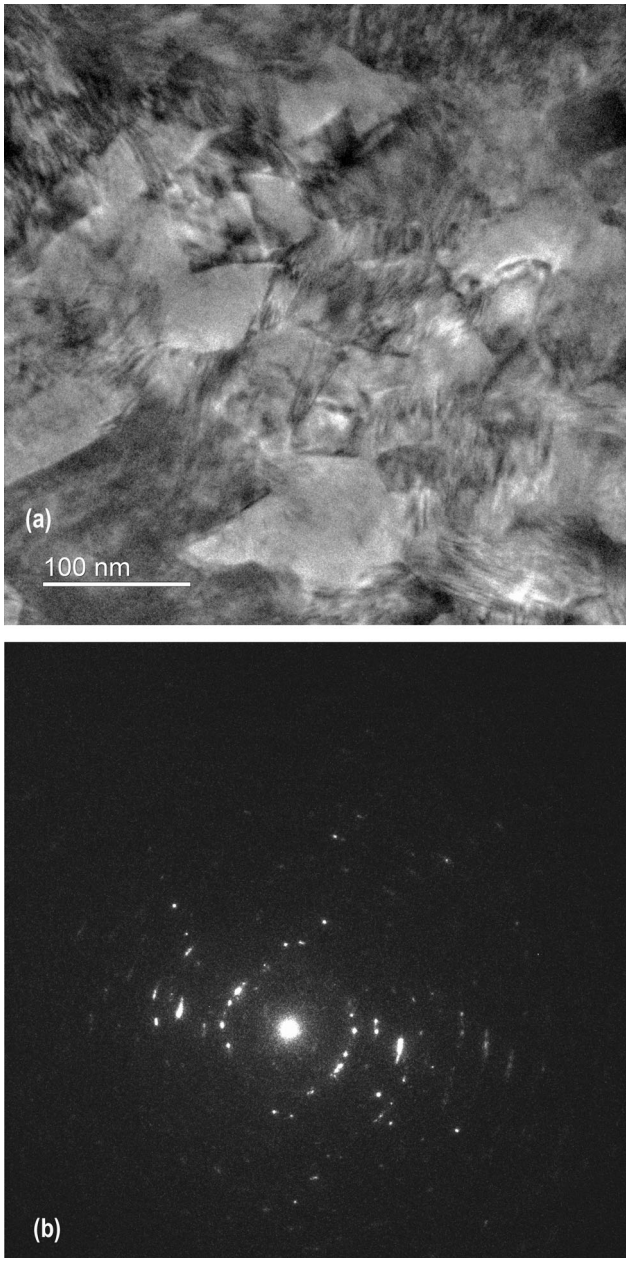

Fig. 6 BF TEM micrograph of the TMAZ prior to creep: (a) BF image; (b) SADP

et al. (Ref 26). However, it is important to remember that despite Matsunaga et al.'s reference to this as a general property of HCP materials, the strain level discussed in their paper, at least in CP-Ti, was markedly lower than the one discussed in the current paper. The TEM study reported here makes it possible to conclude that dislocation glide was the dominant deformation mechanism.

Creep fracture at 600 °C and at 650 °C also occurred at the PM in all cases as well as at 550 °C. This behavior seems to somehow contradict the behavior reported by Long et al. (Ref 25), who studied the compressive deformation behavior of CP-Ti with $\sim$ 35 μm average grain size versus the same material with $\sim$ 250 nm average grain size at temperatures of up to 600 °C. They claimed that when the deformation temperature was higher than the recrystallization temperature, such as in the

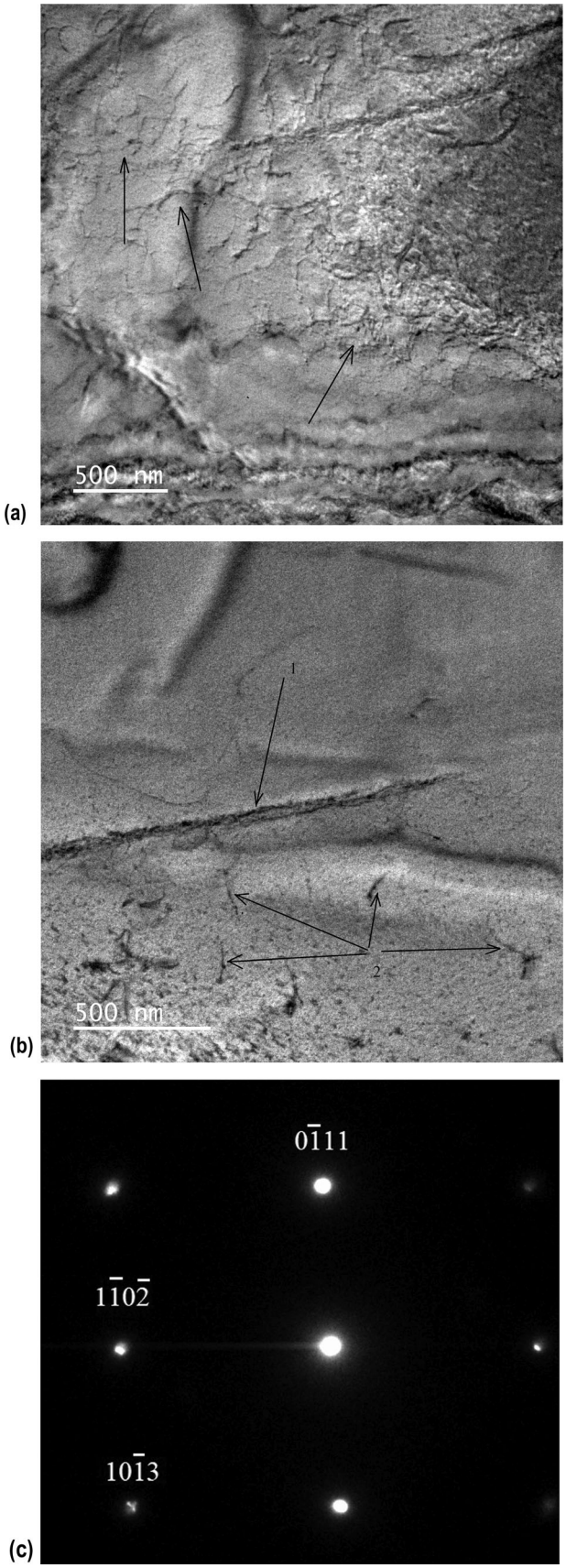

Fig. 7 TEM micrograph of specimen that crept under 12 MPa at 650 °C taken near $< 5\bar{1}\bar{4}3 >$ z.a.: (a,b) BF images; (c) SADP of $< 5\bar{1}\bar{4}3 >$ z.a

case of 600 °C, the coarse grained material exhibited higher creep resistance. They attributed this transition to the contribution of grain boundary sliding and Coble-type creep. The creep tests conducted in the current study showed the opposite, namely that necking and finally fracture always occurred at the coarse grained PM and that the coarse-grained PM showed a lower creep resistance than the nano-sized grains of the TMAZ. Moreover, the conclusion that dislocation glide is the dominant deformation mechanism is in line with Long et al. (Ref 25), who pointed to dislocation glide as the dominant mechanism in the case of their coarse-grained (~35 μm average grain size) material.

The current study showed that under creep conditions, necking and fracturing of the FSW'ed specimens always occurred in the PM, such that the creep resistance of the TMAZ is higher than that of the PM. Keeping in mind that the authors also found that the mechanical properties of the FSWed specimens at room temperature were not inferior to those of the PM (Ref 20), it may be concluded that neither the RT nor the high temperature properties of the FSW'ed material were inferior to those of the PM. The technological implications of the current study together with those of the previous one (Ref 20) are that the welding process has the potential to be regarded as safe for use as far as its mechanical properties are concerned.

4. Conclusions

1. A bead-on-plate FSW was conducted on CP-Ti plates using an H13 tool with a WC pin, instead of a real weld, in order to ensure that the mechanical behavior was solely caused by metallurgical processes and not welding defects, which might cause premature failure.
2. Creep tests were conducted on FSW'ed specimens at 550, 600 and 650 °C, in all cases necking and fracture occurred at the PM indicating, in turn, that the weld with all its subzones is more creep resistant than the parent material.
3. The fracture surfaces investigated were typical of creep fracture, and the fracture mechanism was microvoid coalescence, in addition it ruled out any preexisting defect. This shows, in turn, that the weld was not the weaker link.
4. The TEM study revealed evidence of dislocation glide and dislocation structure formation during creep but not of DRX. It possible to conclude, therefore, that dislocation glide was the dominant deformation mechanism.
5. The results of the current study showing that the creep resistance of the TMAZ is higher than that of the PM together with the results of the previous study showing that the RT properties of the TMAZ were not inferior to those of the PM lead to the claim that FSW of CP-Ti has the potential to be regarded as safe for use.

Acknowledgments

The assistance of N. Navot with welding the material is highly appreciated. The authors thank Dr. E. Kesselman for her assistance with the TEM study and Dr. A. Katz-Demyanetz for his assistance with the SEM study.

Funding

Open access funding provided by Braude College of Engineering. This research project is partially funded by Ort Braude College.

References

1. Y. Zhang, Y.S. Sato, H. Kokawa, S.H.C. Park, and S. Hirano, Stir Zone Microstructure of Commercial Purity Titanium Friction Stir Welded Using pcBN Tool, *Mater. Sci. Eng. A*, 2008, **488**, p 25–30
2. W.B. Lee, C.Y. Lee, W.S. Chang, Y.M. Yeon, and S.B. Jung, Microstructural Investigation of Friction Stir Welded Pure Titanium, *Mater. Lett.*, 2005, **59**, p 3315–3318
3. K. Reshad Seighalani, M.K. Besharati Givi, A.M. Nasiri, and P. Behemat, Investigations on the Effects of the Tool Material, Geometry, and Tilt Angle on Friction Stir Welding of Pure Titanium, *J. Mater. Eng. Perform.*, 2010, **19**, p 955–962
4. H. Fujii, Y. Sun, H. Kato, and K. Nakata, Investigation of Welding Parameter Dependent Microstructure and Mechanical Properties in Friction Stir Welded Pure Ti Joints, *Mater. Sci. Eng. A*, 2010, **527**, p 3386–3391
5. J.D. Kim, E.G. Jin, S.P. Murugan, and Y.D. Park, Recent Advances in Friction-Stir Welding Process and Microstructural Investigation of Friction Stir Welded Pure Titanium, *J. Weld. Join.*, 2017, **35**, p 6–15
6. S. Karna, M. Cheepu, D. Venkateswarulu, and V. Srikanth, Recent Developments and Research Progress on Friction Stir Welding of Titanium Alloys: An Overview, IOP Conf. Ser. Mat. Sci., 2018, 330, 012068 p 1–16
7. N. Xu, Q. Song, Y. Bao, Y. Jiang, J. Shen, and X. Cao, Twinning-Induced Mechanical Properties' Modification of CP-Ti by Friction Stir Welding Associated with Simultaneous Backward Cooling, *Sci. Technol. Weld. Join.*, 2017, **7**, p 610–616
8. S. Bahl, P.L. Nithilaksh, S. Suwas, S.V. Kailas, and K. Chatterjee, Processing–Microstructure–Crystallographic Texture-Surface Property Relationships in Friction Stir Processing of Titanium, *J. Mater. Eng. Perform.*, 2017, **26**, p 4206–4216
9. L. Jiang, W. Huang, C. Liu, L. Chai, X. Yang, and Q. Xu, Microstructure, Texture Evolution and Mechanical Properties of Pure Ti by Friction Stir Processing with Slow Rotation Speed, *Mater Charact*, 2019, **148**, p 1–8
10. B. Callegari, J.P. Oliviera, K. Aristizabal, R.S. Coelho, P.P. Brito, L. Wu, N. Schell, F.A. Soldera, F. Mucklich, and H.C. Pinto, In-situ Synchrotron Radiation Study of the Aging Response of Ti-6Al-4V Alloy With Different Starting Microstructures, *Mater Charact*, 2020, **165**(110400), p 1–10
11. B. Callegari, J.P. Oliviera, R.S. Coelho, P.P. Brito, N. Schell, F.A. Soldera, F. Mucklich, M.I. Sadik, J.L. Garcia and H.C. Pinto, New

Insights into the Microstructural Evolution of Ti-5Al-5Mo-5V-3Cr Alloy During Hot Working, *Mater Charact*, 2020, **162**(110180), p 1–12
12. D.S. Kang and K.J. Lee, Recent R&D Status on Friction Stir Welding of Ti and Its Alloys, *J. Weld. Join.*, 2015, **33**, p 1–7
13. S. Mironov, Y.S. Sato, and H. Kokawa, Development of Grain Structure During Friction Stir Welding of Pure Titanium, *Acta Mater.*, 2009, **57**, p 4519–4528
14. H. Liu, K. Nakata, N. Yamamoto, and J. Liao, Friction Stir Welding of Pure Titanium Lap Joint, *Sci. Technol. Weld. Join.*, 2010, **15**, p 428–432
15. R.W. Fonda, K.E. Knipling, A.J. Levinson, and C.R. Feng, Enhancing the Weldability of CP Titanium Friction Stir Welds with Elemental Foils, *Sci. Technol. Weld. Join.*, 2019, **24**, p 617–623
16. A.K. Singh, L. Kaushik, S. Pawar, J. Singh, H. Das, M. Mondal, S.T. Hong, and S.H. Choi, Unraveling the Heterogeneous Evolution of the Microstructure and Texture in the Thermomechanically Affected Zone of Commercially Pure Titanium During Friction Stir Processing, *Int. J. Mech. Sci.*, 2023, **239**(107894), p 1–15
17. R. Ganesan and H. Pothur, Review on Friction Stir Welding of Titanium Alloys – A fracture Mechanics Perspective. In Advances in Additive Manufacturing and Metal Joining Proceedings of AIMTDR, N. Ramesh Babu, S. Kumar, P.R. Thyla, and K. Sripriyan, Eds., Dec 9-11, 2021, virtual, Springer Nature Singapore Pte Ltd., 2023, p 445-458
18. M. Sajid, G. Kumar, and M. Kumar, Recent Advances in Friction Stir Welding and Processing of Light Metals Alloys, *Int. J. Res. Eng. Innov.*, 2023, **7**, p 15–22
19. H. Liu, Y. Morisada, and H. Fujii, Friction Stir Welding: Process, Temperature, Microstructure and Properties, *Sci. Technol. Weld. Joining*, 2023, **8**, p 619–632
20. M. Regev, B. Almoznino, and S. Spigarelli, A Study of the Metallurgical and Mechanical Properties of Friction-Stir-Welded Pure Titanium, *Metals - Basel*, 2023, **13**, p 5241–52413
21. P. Pushp, S.M. Dasharath, and C. Arati, Classification and Application s of Titanium and Its Alloys, *Mater. Today Proc.*, 2022, **54**, p 537–542
22. K. Gangwar and M. Ranulu, Friction Stir Welding of Titanium Alloys: A Review, *Mater. Des.*, 2018, **141**, p 230–255
23. J. Dvorak, A.G. Kadomtsev, V.I. Betekhtin, V. Sklenicka, P. Kral, M. Kvapilova, Creep Behaviour of Ultrafine - Grained CP Titanium Processed by Multi - Pass Rolling, IOP Conf. Ser. – Mat. Sci., 2021, 1178 012013 p 1-6
24. J. Dvorak, P. Kral, A.G. Kadomtsev, V.I. Betekhtin, M.V. Narykova, M. Kvapilova, and V. Sklenicka, Influence of Cryo-Processing and Post-SPD Annealing on Creep Behavior of CP Titanium, *Materials*, 2022, **15**(1646), p 1–13
25. F.-W. Long, Q.-W. Jiang, L. Xiao, and X.-W. Li, Compressive Deformation Behaviors of Coarse- and Ultrafine-Grained Pure Titanium at Different Temperatures: A Comparative Study, *Mater. Trans.*, 2011, **52**, p 1617–1622
26. T. Matsunaga, T. Kameyama, S. Ueda, and E. Sato, New Creep Region and Mechanism in Hexagonal Close-Packed Metals, *J. Phys. Conf. Ser.*, 2010, **240**(012072), p 1–4
27. S. Spigarelli, M. Regev, A. Santoni, M. Cabibbo, and E. Santecchia, Effect of Friction Stir Welding on Short-Term Creep Response of Pure Titanium, *Metals-Basel*, 2023, **13**, p 1616-1–1616-10
28. W.M. Mahoney, Mechanical Properties of Friction Stir Welded Aluminum Alloys. In Friction Stir Welding and Processing, 1st ed., R.S. Mishra, and W.M. Mahoney, Eds., ASM International: Materials Park, Ohio, USA, 2007; p 72